2025 American Control Conference (ACC)
July 8-10, 2025. Denver, CO, USA

Optimization of Electric Vehicle Evacuation Integrating Mobile Charging Stations and Considering Vehicle Diversity

Xuchang Tang
Simon Kuang
Xinfan Lin*
Dept. of Mech. & Aero. Eng.
University of California, Davis
Davis, California, 95616, USA
lxflin@ucdavis.edu

Shuang Feng
Ricardo de Castro
Dept. of Mech. Eng.
University of California, Merced
Merced, California, 95343, USA

Qijian Gan,
Scott Moura
California PATH
University of California, Berkeley
Berkeley, California, 94720, USA

***Abstract*—This paper addresses the challenges of electric vehicles (EVs) long-distance mass evacuations, particularly those posed by the extended charging time. We focus on optimizing evacuation planning in high EV ownership areas by considering route selection, vehicle grouping, departure timing, and charging scheduling, while incorporating Mobile Charging Stations (MCS) to supplement the existing Fixed Charging Stations (FCS). A two-stage optimization approach is used, i.e. route optimization through a recursive Dijkstra algorithm, followed by vehicle scheduling and MCS deployment via Mixed Integer Linear Programming (MILP). Apart from demonstrating the effectiveness of MCS in reducing the evacuation time, the study reveals key insights on the optimal scheduling and MCS placement patterns. In addition, this paper also investigates the impact of nonuniform properties (such as battery sizes and initial energy level) among EVs on the evacuation time, relating to the more complicated real-world operating conditions. Furthermore, through quantifying the impact of infrastructure capacities on evacuation, specifically charging rate and traveling speed, insights on cost-effective resource allocation for infrastructure upgrade are generated. The outcome provides a valuable tool for local agencies to optimize and evaluate evacuation strategies and infrastructure, with results showcasing the significant potential of MCS in enhancing EV evacuations in high-risk regions.**

***Index Terms*—Electric Vehicle, Emergency Evacuation, Mobile Charging Station**

I. INTRODUCTION

The frequency of large-scale community evacuations due to natural disasters is on the rise. In California, wildfires are a common threat because of the region's unique climate. Several recent wildfires have necessitated massive evacuations. For example, the 2018 Camp Fire led to the evacuation of approximately $52,000$ residents in the Town of Paradise [1], while the 2019 Kincade Fire forced nearly $200,000$ people to evacuate in Sonoma County, with a state of emergency declared [2]. Hurricanes are another major cause of widespread evacuations. In 2017, Hurricane Irma triggered the evacuation of over 6 million people across Florida, Georgia, and South Carolina [3]. During this event, personal vehicles played a crucial role, with over half of the $170,000$ surveyed evacuees traveling more than 50 miles [4].

Mass electric vehicle (EV) evacuation presents several challenges. The charging infrastructure in the U.S. has not kept pace with the EV adoption, as the vehicle-to-charger ratio is currently at 17 [5], and the rapid growth of EVs is further outpacing the Fixed Charging Station (FCS) construction [6]. The uneven distribution of FCSs exacerbates the issue, disproportionately affecting disadvantaged communities [7], [8]. Even if more stations are built, their locations will most likely be planned for daily usage rather than the demands of mass evacuation. Another challenge is the significantly longer charging time of EVs compared to the refueling of gasoline vehicles. In North America, Level 1 chargers provide approximately 5 miles of range per hour, Level 2 offers 10-20 miles per hour, and Level 3 (DC fast charging) can charge up to 80% in 30 minutes [9], [10]. In contrast, gasoline vehicles refuel in under 10 minutes. Such disparity further complicates the long-distance EV travel in emergency situations, adding to the difficulty caused by limited availability of charging.

During evacuations, vehicles are grouped based on similar characteristics, such as departure state-of-charge (SOC), battery size, and synchronized evacuation instructions.

The primary objective of evacuation is to ensure that all vehicles and the population can reach safety within the shortest or an acceptable amount of time. Evacuation planning needs to address the following aspects of the operation, including (1) The optimal number of vehicles in each evacuation group, (2) The best time for each group to begin their journey, (3) The most efficient routes for each group to follow, and (4) The locations for vehicles to stop for refueling or recharging.

Several recent studies have explored evacuation planning for EVs [11]–[15]. For instance, in [14], EV-only evacuation

*Corresponding author
This work is supported by the California Climate Action Seed Grants of the University of California (Grant No.R02CP6996)

scenarios are addressed by formulating a three-stage approach. The procedures included consolidating the network by pre-assigning charging stations, ranking node significance based on key paths, and solving the evacuation plan as a mixed-integer linear programming problem aimed at minimizing the total evacuation time. In [15], the researchers modeled the evacuation route planning problem as a minimum spanning tree with hop constraints and minimized total evacuation time using a branch-and-price heuristic algorithm. Their numerical results demonstrated enhanced evacuation performance with denser and strategically placed charging infrastructures, highlighting the potential need for more charging stations during emergency evacuations.

Most existing studies on EV evacuation planning identify limited charging station availability as a major bottleneck, with infrastructure expansion being costly and time-consuming. To address this, we introduce Mobile Charging Stations (MCS) as a flexible, cost-effective solution. MCSs, such as battery-equipped trucks [16], [17], provide charging at critical times and locations, ensuring availability during mass evacuations when demand spikes and the power grid may be unreliable. This work builds on our previous study [18], which first proposed using MCS in EV evacuation scenarios.

In our methodology, a multi-layer framework is formulated to perform key optimization tasks including route selection, vehicle grouping, and scheduling for both departures and charging times. By incorporating MCS placement into the evacuation schedule, the framework aims to minimize total evacuation time.

This paper contributes to evacuation planning optimization by addressing non-uniform EV properties, such as varying battery sizes and at-departure energy levels. This enhancement reflects real-world complexities, and its impact on planning results is analyzed. Additionally, we assess how infrastructure capacities, specifically charging rates and road travel speeds, influence total evacuation time. By evaluating different scenarios, our findings offer insights into cost-effective infrastructure upgrades, guiding whether to prioritize road expansion or charging power enhancement to improve EV evacuation preparedness.

II. Methodology

A. Problem Statement

A network $G(\mathbb{N}, \mathbb{E})$ is a mathematical structure used to model the geography of an area of interest. $\mathbb{N}$ is the set of nodes that represents physical locations in the map. $\mathbb{E}$ is the set of edges that defines the connection and travel cost (in our case, we consider travel time and energy) between nodes.

Given an origin-destination (OD) location pair $w = (n_o, n_d)$, with $n_o, n_d \in \mathbb{N}$ representing the origin and destination, respectively, in a network $G(\mathbb{N}, \mathbb{E})$, a set of vehicle-specific evacuation demand information I_{vhc}, and the number of available MCS(s) with its (their) set of information I_{mcs}, the objective is to find the optimal decision on routing (waypoint and charging location selection), vehicle grouping, departure scheduling, and MCS placement such that the summed evacuation time for all vehicles is minimized.

To achieve the goal, the process is divided into two stages to simplify the optimization procedures, as illustrated in Figure 1. In Stage 1, the focus is on identifying feasible routes, which consists of traveling waypoints and charging locations. Stage 2 addresses vehicle grouping, departure time scheduling, route assignment, and mobile charging stations (MCS) location placement.

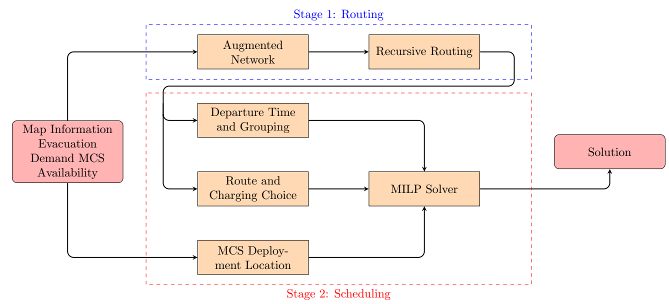

Fig. 1. Evacuation Planning and Optimization based on Two-Stage Approach

We assume all users adhere strictly to the instructions, although this is not typical in real-life scenarios. In our two-stage process, vehicles are not allowed to queue at charging stations and will remain at their origin until instructed to depart. The power grid is assumed to remain fully operational throughout the evacuation. MCS are deployed only once at the start of the evacuation with fully charged batteries, and all MCS and FCS ports share the same charging rate. We assume there is no traffic delay due to congestion.

B. Routing

Given a network $G(\mathbb{N}, \mathbb{E})$ consisting of a set of nodes $\mathbb{N}$ and edges $\mathbb{E}$, the objective is to identify the K shortest paths between the OD pair, denoted as $\{p_0, \cdots, p_{K-1}\}$. A valid path p is defined as a sequence of nodes connected by edges. Additionally, the state of charge (SOC) of vehicles, traveling along any path p_i must remain within a specified range $soc_t \in [\underline{soc}, \overline{soc}]$ for all time instants $t \in \mathbb{T}$, where $\mathbb{T}$ represents the set of all instants. The SOC refers to the ratio of the vehicle's remaining energy to its battery capacity, expressed as a percentage [19], [20].

To construct the optimization framework, the network's cost matrices are first established. In the network G, nodes $\mathbb{N}$ represent intersections and key locations, while edges $\mathbb{E}$ model the roads connecting these nodes. The adjacency matrix A defines node connectivity, where $A_{n_i,n_j} = 1$ indicates a direct connection between nodes n_i and n_j.

The network G is associated with three primary cost matrices: distance (C^d), time (C^t), and energy (C^e). The distance cost matrix C^d captures the Euclidean distance between connected nodes. The time cost matrix C^t is determined by dividing the distance by the vehicle speed v_{ij}, $C^t_{ij} = \frac{C^d_{ij}}{v_{ij}}$. Similarly, the energy cost matrix C^e is computed by dividing the distance by the energy consumption rate η_{ij}, such that $C^e_{ij} = \frac{C^d_{ij}}{\eta_{ij}}$. If there is no direct connection between nodes n_i and n_j (i.e.,

$A_{ij} = 0$), the corresponding cost entry is set to ∞ in all matrices to reflect the lack of a viable path.

In the context of EV evacuation, charging behavior is incorporated by augmenting the original network $G(\mathbb{N}, \mathbb{E})$. The schematic is shown in Figure 2. This augmentation treats charging as traveling along an edge with a negative energy cost (reflecting an increase in state of charge, SOC). The augmented network, denoted as $\tilde{G}$, includes nodes representing both fixed charging stations (FCS) and potential mobile charging station (MCS) deployment sites. For each charging-capable node n_i, a set of virtual nodes $\{\tilde{n}_{i,1}, \cdots, \tilde{n}_{i,k}, \cdots, \tilde{n}_{i,N_\%}\}$ is appended, where each virtual node represents a specific SOC target (e.g., 50%, 75%, 100%) and $N_\%$ represents the total number of charging choices.

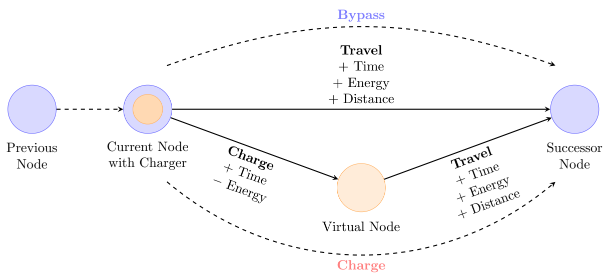

Fig. 2. Using Virtual Nodes to Represent Charging Behavior

Upon arrival at a charging node, vehicles can either skip charging and continue on their route, or "drive" to one of the virtual nodes, accruing a positive time cost and a negative energy cost. Once charging is complete, the vehicle resumes travel toward the next real node.

The augmented adjacency matrix $\tilde{A}$ maintains the structure of the original adjacency matrix A in its upper-left portion. For any physical node n_i connected to a virtual charging node $\tilde{n}_{i,k}$, a new entry $\tilde{A}_{n_i,\tilde{n}_{i,k}} = 1$ is added. Similarly, for each successor physical node $n_j \in succ\{n_i\}$ in the original network, an entry $\tilde{A}_{\tilde{n}_{i,k},n_j} = 1$ is introduced, allowing vehicles to proceed after charging. The cost matrices are also extended, with new elements $\tilde{C}_{\tilde{n}_{i,k},n_j} = C_{n_i,n_j}$, and $\tilde{C}_{n_i,\tilde{n}_{i,k}}$ reflects the charging cost.

Building on the foundation of the augmented network and the grouping of vehicles with similar parameters, we integrate charging behavior into the network model to optimize both travel and charging decisions during evacuation. This approach allows the application of path-finding algorithms, such as Dijkstra's Algorithm, directly within the framework while incorporating state-of-charge (SOC) constraints. The objective is to minimize travel time, using it as a positive edge weight, while ensuring energy feasibility throughout the evacuation route.

Since Dijkstra's Algorithm is a greedy algorithm, applying it with the same initial conditions and map will produce identical outcomes. To introduce variability and explore alternative solutions, we mask combinations of virtual nodes—each representing different charging options—and run the path-finding algorithm multiple times. This technique enables the efficient identification and ranking of the K shortest paths.

C. EV Evacuation Scheduling and MCS Placement

For each origin-destination (OD) pair $w(n_o, n_d)$ in the full set $\mathbb{W}$, and given the set of available paths $\mathbb{P}_w$ between the OD pairs (from routing), the objective is to determine the optimal vehicle departure times and mobile charging station (MCS) locations in such a way that the total evacuation time for all vehicles is minimized. We define a demand to be a tuple $w_d = (n_{o,w}, n_{d,w}, f_w)$, where $n_{o,w}$ and $n_{d,w}$ are the origin and destination of OD-pair w, respectively, and f_w is the number of vehicle that require a planned evacuation from $n_{o,w}$ to $n_{d,w}$.

We adopt a discrete time representation where time $t \in \mathbb{T}$ takes non-negative integer values. The problem of scheduling vehicle departures and deploying mobile charging stations (MCS) is formulated as a mixed-integer linear programming (MILP) model, which is then solved using the Gurobi optimizer [21].

The MILP formulation involves several key decision variables. The integer variable x_{wpt} represents the number of electric vehicles (EVs) departing from an origin-destination pair w, following path p, and departing at time t. Furthermore, the deployment of mobile charging stations (MCS) is modeled using the binary variable q_{mn}, where $q_{mn} = 1$ indicates the presence of the m-th MCS at node n, while $q_{mn} = 0$ denotes its absence. These decision variables allow for the optimization of both vehicle routing and MCS deployment in the evacuation process.

The objective of the optimization is to minimize the total evacuation time for all vehicles. This is expressed as the sum of the departure time and the total travel and charging time for each vehicle. Mathematically, the objective is formulated as:

$$\sum_{w \in \mathbb{W}} \sum_{p \in \mathbb{P}_w} \sum_{t \in \mathbb{T}} (t + \tilde{t}_{wpt}) \times x_{wpt}, \tag{1}$$

where $\tilde{t}_{wpt}$ represents the pre-calculated total travel and charging time for a vehicle departing from origin-destination pair w, following path p, at time t. The variable x_{wpt} denotes the number of vehicles assigned to each route and departure time. By minimizing this sum, the model ensures that the overall evacuation process is optimized in terms of time efficiency.

Several critical constraints must be considered to ensure the plausibility of the evacuation planning.

The evacuation demand constraint ensures that all vehicles assigned to a specific origin-destination (OD) pair are evacuated. This is expressed by the equation:

$$\sum_{p \in \mathbb{P}w} \sum_{t \in \mathbb{T}} x_{wpt} = f_w, \; \forall w \in \mathbb{W} \tag{2}$$

where f_w represents the total demand (number of vehicles) that require planned evacuation from origin $n_{o,w}$ to destination $n_{d,w}$. The sum of vehicles evacuated along all paths p and departure times t must be equal to f_w for each OD pair.

The single-site MCS deployment constraint ensures that each mobile charging station (MCS) is deployed at no more than one node at any given time. This is governed by the equation:

$$\sum_{n \in \mathbb{N}} q_{mn} = 1, \forall m \in \mathbb{M}, \tag{3}$$

indicating for each MCS m, the summation across all node of its binary deployment index $q_m n$ can only equal to 1.

The port limit constraint ensures that the demand for charging ports does not exceed the available supply at any node and time. This is expressed by:

$$D_{nt} \leq S_{nt}, \forall n \in \mathbb{N}, \forall t \in \mathbb{T}, \tag{4}$$

where D_{nt} is the charging demand at node n at time t, and S_{nt} is the corresponding supply of charging ports.

Finally, the MCS energy constraint ensures that the state of charge (SOC) of each MCS remains within acceptable bounds, represented by the equation:

$$0 \leq soc_{mt} \leq 1, \forall m \in \mathbb{M}, \forall t \in \mathbb{T} \tag{5}$$

This constraint bounds the SOC of each MCS m between 0% and 100% at any time t.

Energy tracking for MCS and the coupling between MCS and EV energy are managed through an expanded set of linear programming constraints, which are not included in this paper due to space limitations. These constraints ensure effective evacuation scheduling, optimal deployment of charging infrastructure, and efficient energy resource management throughout the evacuation process. Additional details on the auxiliary variables used in the MILP formulation are available in the study by Tang et al. [18].

III. Case Study

We selected a modified map of Sioux Falls for our case study. The map is based on the geography of the region but with extended range, and is frequently used in similar studies [15], [22]. The abstract network is shown in Figure 3, with evacuation origin (danger), destination (safety), and permanent chargers (FCS) marked.

Each FCS is equipped with 50 charging ports, with some nodes having multiple FCSs, and each MCS with 20 charging ports and a 420 kWh battery. The evacuation demand (# of EVs to evacuate) and the number of existing charging ports at each node are listed in Table I. We consider a hypothetical disaster affecting node 13, and all vehicles in the node are required to evacuate to node 2 through the area. There are a total of $1,460$ vehicles registered for evacuation, and a total of 800 charging ports from existing FCSs. The longitudinal (East-West) range is 370 km, and the latitudinal (North-South) range is 460 km. The evacuation Manhattan distance from node 13 to node 2 is 730 km. We assume all vehicles charge to 100% when stopping at a charging station. This assumption will be relaxed in future work.

Regarding vehicle parameters, we consider the battery capacity (corresponding to vehicle range) and at-departure SOC to be nonuniform, and distributed in various combinations among vehicles as shown in Table II. There are a total of 9 combinations representing vehicles with short, medium, and long ranges as well as low, medium, and high initial energy levels, with each combination containing the same number of vehicles. More combinations with finer granularity in distribution can be included if necessary. Meanwhile, as a baseline for comparison, we also consider a case where the vehicle parameters are uniform. In this case, all vehicles have

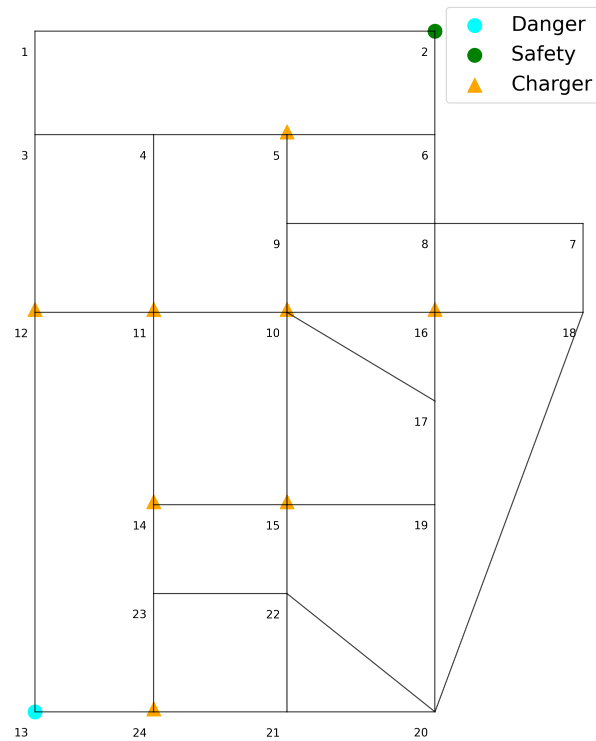

Fig. 3. Modified Map of the City of Sioux Falls

TABLE I
EVACUATION DEMAND AND FCS PORTS ALLOCATION

Node Label	# EVs to evacuate	FCS Ports	Node Label	# EVs to evacuate	FCS Ports
1	-	-	13	$1,460$	-
2	-	-	14	-	200
3	-	-	15	-	150
4	-	-	16	-	50
5		50	17	-	-
6	-	-	18	-	-
7	-	-	19	-	-
8	-	-	20	-	-
9	-	-	21	-	-
10	-	150	22	-	-
11	-	50	23	-	-
12	-	50	24	-	100

TABLE II
POSSIBLE VEHICLE PARAMETERS

At-departure SOC	50%	75%	100%
Battery size (kWh)	80	100	120

75% at-departure SOC and 100 kWh battery capacity, which are the mean values of the combinations in the uniform case.

Other parameters are considered to be uniform among vehicles or charging stations. Specifically, the charging rate is fixed at 48 kW for all chargers and traveling speed at 50 mph for all vehicles (before applying the time-varying delay ratio). However, we will vary these two parameters over a range of values in later sections to investigate their impacts on the results.

IV. Results and Discussions

A. Reduction in Evacuation Time

We evaluate the efficacy of an evacuation result using the metric of the average evacuation time (equivalent to the total evacuation time). It is the average time for all vehicles to arrive at the destination since the beginning of evacuation. The results are shown in Figure 4 for different cases under different number of MCSs.

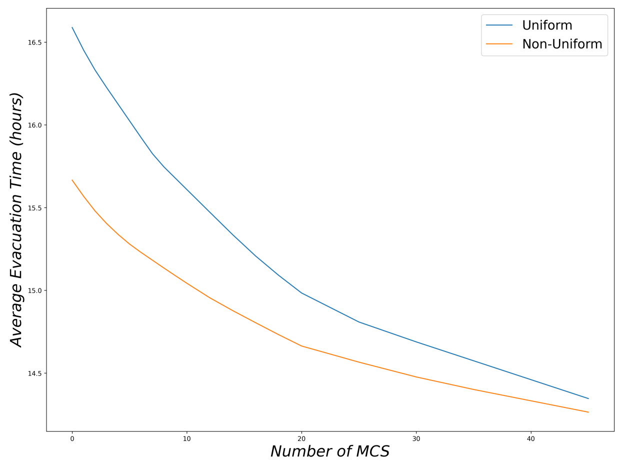

Fig. 4. Evacuation Time versus number of MCSs

It is seen that adding MCS could significantly reduce the evacuation time. For example, for the simpler case with uniform vehicle parameters, by adding only 5 MCSs, the average can be reduced by 3.5%, compared to the scenario with no MCS. When further increasing the number of MCSs to 40, the reduction in average evacuation time grows to 13%. For the more complicated case of non-uniform vehicle parameters, compared with the scenario with no MCS, when deploying only 5 MCSs, the average can be reduced by 2.5%, and with 40 MCSs, the average evacuation time reduction becomes 9.5%.

Regarding the effect of non-uniform distribution of EV battery sizes (ranges) and at-departure SOCs, it is seen that the average evacuation time is in general lower than that in the uniform case. This might be explained by the fact that the scarcity of charging stations is the main limiting factor in evacuation time. In the nonuniform case, the presence of vehicles with less charging demand, i.e. those with high range and high initial SOC, will alleviate the pressure on the charging stations. This is supported by the trend shown in Fig. 4, where the difference between the two cases decreases as the number of MCSs increases. The results also demonstrate the effectiveness of MCSs in accommodating the diversity in EV types and their initial conditions typical in the real-world evacuation scenario.

B. Scheduling Behavior

Figures 5 and 6 illustrate the distribution of EV group sizes (with 1 MCS) under both uniform and non-uniform battery capacities and initial SOCs. The green ticks represent the number of ports in a Mobile Charging Station (MCS), red ticks denote the number of ports in a Fixed Charging Station (FCS), and orange ticks indicate the combined number of ports when one MCS is integrated with multiple FCS.

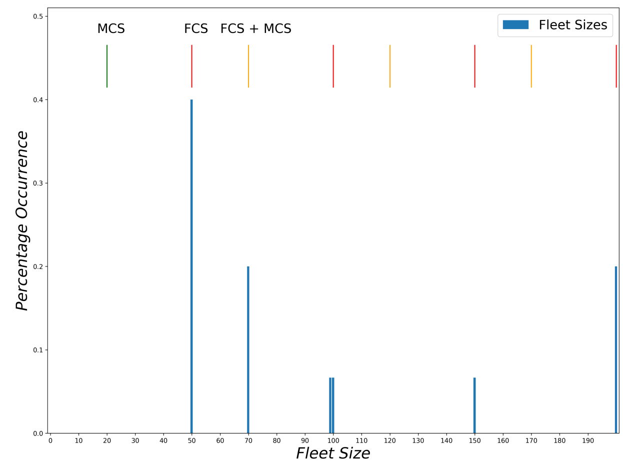

Fig. 5. EV Group Size Distributions under Uniform EV Parameters with 1 MCS

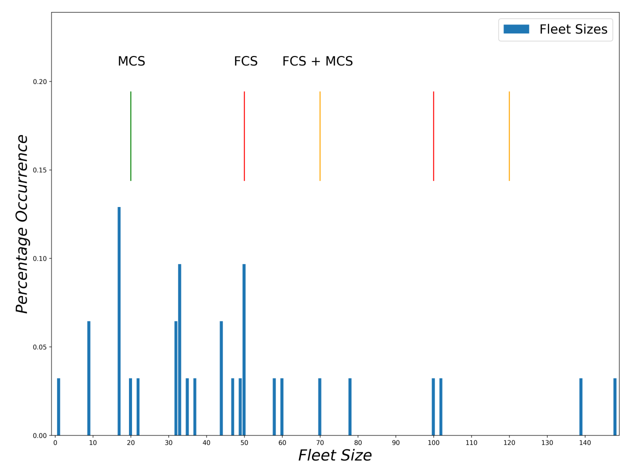

Fig. 6. EV Group Size Distributions under Non-uniform EV Parameters with 1 MCS

In the uniform case, it is seen that the highest peak occurs at the group size of 50, accounting for 40% of the groups. It is interesting to note that 50 is the set number of available ports per fixed charging station. Other values of popular group sizes, such as those at 70, 100, and 150, are either multiples of the number of ports at FCS or MCS or their combinations. Such correlation between group size distribution and the charging port numbers can be explained by the fact that the optimal scheduling needs to maximize the charging port usage. Therefore, one heuristic is to match the number of vehicles in a group with that of available ports.

Meanwhile, in the non-uniform case, the distribution of vehicle group sizes exhibits a more dispersed pattern, with the highest peak significantly lower at 0.13. Additionally, a wider range of group sizes show up in the distribution. This outcome is expected because variation in EV battery capacity and initial SOCs results in different charging durations, even when vehicles follow the same evacuation route. As optimal scheduler tends to maximize the usage of available ports, smaller "fill-in" groups need to be dispatched in order to make full use of the available port time, resulting in a more diverse distribution of group sizes.

C. Impacts of Traveling and Charging Speeds

To evaluate the impact of infrastructure capacities on evacuation performance, the optimization is repeated with charging rates ranging from $5\ kW$ to $350\ kW$ and vehicle speeds from $25\ mph$ to $85\ mph$. This sensitivity analysis examines how charging rates and travel speeds affect average evacuation time, providing insights into regional infrastructure effectiveness. Figure 7 presents a 3D plot illustrating these effects, with the z-axis representing time in hours.

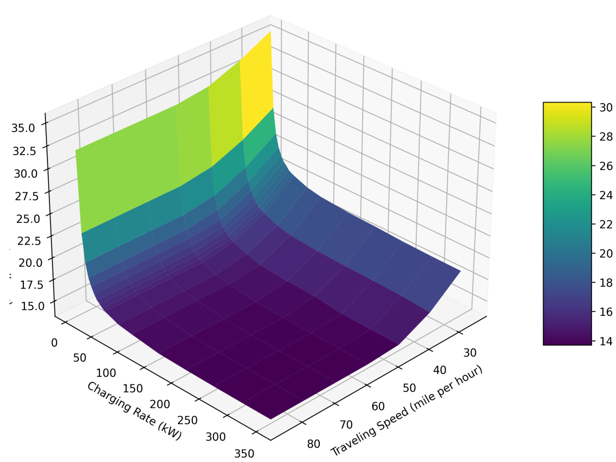

Fig. 7. Average Evacuation Time under Different Charging Rates and Vehicle Traveling Speeds for Uniform EV Parameter Case)

It is seen that the average evacuation time decays nearly exponentially as either charging rate or traveling speed increases. The curve begins to flatten when the charging rate exceeds $50\ kW$ and the traveling speed surpasses $45\ mph$. The information could aid the local agencies to make decisions on infrastructure upgrade, i.e. given the current charging and transportation capacities, whether it is more cost effective to improve the road or charging facilities.

Furthermore, we can extract the contour plots under certain fixed (target) average evacuation as shown in Fig. 8. Taking the evacuation time of 15 hours as an example, the contour line shows all combinations of charging rates and traveling speed that could complete the evacuation within the target time. It would also be interesting to see how the plot will change under different number of MCSs, which could reveal how adding MCSs could improve the overall cost effectiveness by reducing the need for the much more expensive infrastructure upgrade (expanding road, grid, or installing more FCSs permanently).

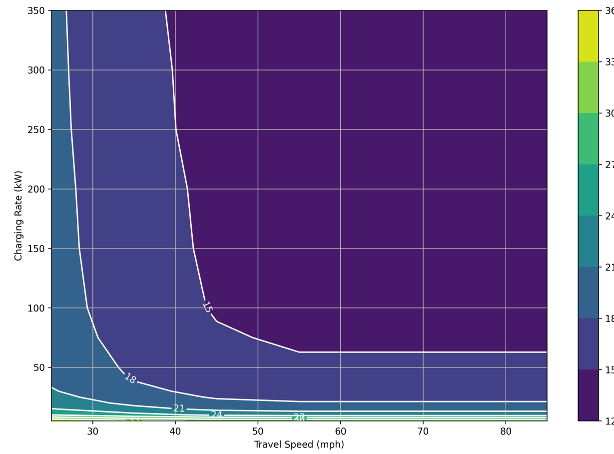

Fig. 8. Traveling Speed versus Charging Rate Contour Plots under Fixed Average Evacuation Time

V. Conclusion

In this paper, we explore electric vehicle (EV) evacuation planning with the aid of mobile charging stations (MCSs), using a modified Sioux Falls map as a case study. In particular, we take into account the diversity of parameters among vehicles, including nonuniform EV battery sizes (range) and at-departure SOC. The findings reveal several key insights. First, increasing the number of MCSs effectively reduces the evacuation time, in both uniform and nonuniform EV parameters cases, highlighting the potential of MCSs to enhance evacuation efficiency. Second, the difference in evacuation time between the uniform and nonuniform EV parameter cases decreases as the number of MCSs increases, revealing the effectiveness of MCSs in accommodating the real-world complexity of vehicle diversity. Third, the optimal vehicle group sizes are closely related to the number of charging ports at charging stations, suggesting that the availability of charging ports plays a critical role in determining the best grouping strategy for vehicles. Furthermore, in the nonuniform EV parameter case, the distribution of group sizes is more diverse compared with the uniform case, indicating that grouping with finer granularity is needed when dealing with real-world EV diversities. Finally, the impacts of infrastructure parameters, e.g. traveling speed and charging power rate, on evacuation time are also analyzed, which could provide useful insights for decision making on infrastructure upgrade to better prepare for evacuation operation.

References

[1] A. Maranghides, W. E. Mell, S. Hawks, M. Wilson, W. Brewer, E. Link, C. Brown, C. Murrill, and E. Ashley, *Camp Fire Preliminary Reconnaissance*. US Department of Commerce, National Institute of Standards and Technology, 2020.

[2] S. D. Wong, J. C. Broader, and S. A. Shaheen, "Review of california wildfire evacuations from 2017 to 2019," report, University of California Institute of Transportation Studies (UC ITS), 2020.

[3] S. Wong, S. Shaheen, and J. Walker, "Understanding evacuee behavior: A case study of hurricane irma," report, University of California, Berkeley, Transportation Sustainability Research center, 2018.

[4] H. Younes, A. Darzi, and L. Zhang, "How effective are evacuation orders? an analysis of decision making among vulnerable populations in florida during hurricane irma," *Travel behaviour and society*, vol. 25, pp. 144–152, 2021.

[5] S. Á. Funke, F. Sprei, T. Gnann, and P. Plötz, "How much charging infrastructure do electric vehicles need? a review of the evidence and international comparison," *Transportation research part D: transport and environment*, vol. 77, pp. 224–242, 2019.

[6] T. Nogueira, E. Sousa, and G. R. Alves, "Electric vehicles growth until 2030: Impact on the distribution network power," *Energy Reports*, vol. 8, pp. 145–152, 2022.

[7] M. Nicholas, D. Hall, and N. Lutsey, "Quantifying the electric vehicle charging infrastructure gap across us markets," *International Council on Clean Transportation*, vol. 20, pp. 1–39, 2019.

[8] M. Nazari-Heris, A. Loni, S. Asadi, and B. Mohammadi-ivatloo, "Toward social equity access and mobile charging stations for electric vehicles: A case study in los angeles," *Applied Energy*, vol. 311, p. 118704, 2022.

[9] M. S. Mastoi, S. Zhuang, H. M. Munir, M. Haris, M. Hassan, M. Usman, S. S. H. Bukhari, and J.-S. Ro, "An in-depth analysis of electric vehicle charging station infrastructure, policy implications, and future trends," *Energy Reports*, vol. 8, pp. 11504–11529, 2022.

[10] S. Hardman, A. Jenn, G. Tal, J. Axsen, G. Beard, N. Daina, E. Figenbaum, N. Jakobsson, P. Jochem, N. Kinnear, *et al.*, "A review of consumer preferences of and interactions with electric vehicle charging infrastructure," *Transportation Research Part D: Transport and Environment*, vol. 62, pp. 508–523, 2018.

[11] K. Feng, N. Lin, S. Xian, and M. V. Chester, "Can we evacuate from hurricanes with electric vehicles?," *Transportation research part D: transport and environment*, vol. 86, p. 102458, 2020.

[12] L. Lu, *Designing electric vehicle charging infrastructure to enable disaster evacuation*. PhD thesis, University of Texas at Austin, 2022.

[13] J. Zhang and X. Zhang, "A multi-trip electric bus routing model considering equity during short-notice evacuations," *Transportation Research Part D: Transport and Environment*, vol. 110, p. 103397, 2022.

[14] Q. Li, S. Soleimaniamiri, and X. Li, "Optimal mass evacuation planning for electric vehicles before natural disasters," *Transportation research part D: transport and environment*, vol. 107, p. 103292, 2022.

[15] D. S. D. Purba, E. Kontou, and C. Vogiatzis, "Evacuation route planning for alternative fuel vehicles," *Transportation research part C: emerging technologies*, vol. 143, p. 103837, 2022.

[16] S. Afshar, P. Macedo, F. Mohamed, and V. Disfani, "Mobile charging stations for electric vehicles—a review," *Renewable and Sustainable Energy Reviews*, vol. 152, p. 111654, 2021.

[17] Y. Zhang, X. Liu, W. Wei, T. Peng, G. Hong, and C. Meng, "Mobile charging: A novel charging system for electric vehicles in urban areas," *Applied Energy*, vol. 278, p. 115648, 2020.

[18] X. Tang, X. Lin, S. Feng, S. Markolf, R. de Castro, Q. Gan, and S. Moura, "Enhancing large-scale evacuations of electric vehicles through integration of mobile charging stations," in *Proceedings of the IEEE ITSC 2024 Conference*, IEEE, 2024. Accepted, forthcoming publication.

[19] X. Lin, Y. Kim, S. Mohan, J. B. Siegel, and A. G. Stefanopoulou, "Modeling and estimation for advanced battery management," *Annual Review of Control, Robotics, and Autonomous Systems*, vol. 2, no. 1, pp. 393–426, 2019.

[20] X. Lin, H. E. Perez, S. Mohan, J. B. Siegel, A. G. Stefanopoulou, Y. Ding, and M. P. Castanier, "A lumped-parameter electro-thermal model for cylindrical batteries," *Journal of Power Sources*, vol. 257, pp. 1–11, 2014.

[21] Gurobi Optimization, LLC, "Gurobi Optimizer Reference Manual," 2024.

[22] X. Sun, Z. Chen, and Y. Yin, "Integrated planning of static and dynamic charging infrastructure for electric vehicles," *Transportation Research Part D: Transport and Environment*, vol. 83, p. 102331, 2020.